ORIGINAL PAPER

The feasibility of using ethylene-vinyl acetate/natural rubber (EVA/NR)-based thermoplastic elastomer as filament material in fused deposition modelling (FDM)-3D printing application

Dayang Habibah Abang Ismawi Hassim[1] · Nik Intan Nik Ismail[1] · Siti Salina Sarkawi[1] · Yen Wan Ngeow[1] · Suhawati Ibrahim[1] · Kok Chong Yong[1]

Abstract

A series of ethylene-vinyl acetate/natural rubber (EVA/NR)-based thermoplastic elastomer (TPE) blends were developed for fused deposition modelling (FDM)-3D printing application. Two types of the EVA, namely EVA20 (17–20% vinyl acetate) and EVA24 (24–27% vinyl acetate), were used. The grafted EVA was blended with NR in various ratios using a melt blending approach. The effect of EVA/NR blends ratios were studied for thermal, melt flow index, mechanical and dynamic properties. Differential Scanning Calorimetry (DSC) analysis showed that increasing the NR ratio decreased the crystallinity of EVA/NR blends. Similarly, the melt flow index, hardness and tensile strength also reduced as NR content increased in the EVA blends. Printability study indicated that both EVA20 and EVA24 with their blends experienced buckling problems due to insufficient strength and stiffness for acting as push rods for the filament extrusion. Further investigation revealed that the elastic modulus (E') and loss modulus (E'') of EVA/NR blend was lower indicating lower stiffness and viscous response compared to commercial Thermoplastic Urethane and Nylon filaments. The feasibility study of EVA/NR blend in 3D printing provide fresh insight to develop TPE blends as potential 3D printing materials, especially involving natural rubber.

Keywords Ethylene-vinyl acetate · Natural rubber · Thermoplastic elastomer · 3D printing · Fused deposition modelling · Blends

Introduction

Fused deposition modelling (FDM) is an additive manufacturing technique wherein molten polymer filaments are extruded and deposited in a 'layer-by-layer' technique which can produce complex 3D products [1]. Standard rigid thermoplastic materials, i.e. (acrylonitrile–butadiene–styrene copolymer (ABS), nylon, poly(lactic acid) (PLA) and polyethylene terephthalate (PET) are commercially available as FDM feedstock materials. Flexible filaments are recently being explored as new material in 3D printing. Currently, most flexible filaments are based on thermoplastic urethane (TPU) [2]. Feedstock materials for flexible TPE filaments with good mechanical properties have been scarce in the

FDM process [3, 4]. Several issues have been encountered by researchers during extrusion in developing flexible filaments using the FDM technique, and the most common is the incompatibility of current FDM machine with flexible filaments [3]. Non-homogeneous mixing and weak matrix–filler interactions can contribute to poor 3D interlayer adhesion. Furthermore, difficulties in controlling process temperature during filament fabrication can cause polymer swelling and material degradation [5]. Due to that, for commercial flexible filaments, Lehmann et al. [6] suggested custom-made items/commercial parts for the modifications of 3D printer nozzle, hot-end and process parameter adjustments to optimise printing results.

Further developments on flexible filaments are thus required to fully utilise FDM technology for a wide range of product applications. Thermoplastic elastomer (TPE), with rubber-like properties, has gained interest as an FDM feedstock. The mechanical properties of FDM parts are often inferior to those of conventional injection moulded parts [7]. Recently, pellet additive manufacturing (PAM)

✉ Nik Intan Nik Ismail
nikintan@lgm.gov.my

[1] Engineering and Technology Division, Malaysian Rubber Board (MRB), 47000 Sg. Buloh, Selangor, Malaysia

technology for 3D printers to produce soft TPE was developed [8]. Using the right TPE material and process parameters, mechanical properties up to 50% of the values of comparable injection moulded parts can be achieved.

Ethylene-vinyl acetate (EVA) is a material which exhibits excellent toughness and low melting point, which making it a possible candidate for flexible parts in FDM application [9]. On the other hand, as thermoset material, NR is less suitable for FDM. Therefore, an EVA/NR blend would be a suitable combination for filament as the EVA can be used as its thermoplastic carrier. Due to their different polarities, EVA and NR have been reported to be immiscible [10, 11]. The properties of EVA are dependent on vinyl acetate content, molecular branching, molecular weight and distribution [12]. Previous studies [11, 13] on EVA/NR blend properties have shown that increasing NR ratio decreased tensile strength, probably due to the decreasing crystallinity of the EVA phase in the blended compound. This drawback in the EVA/NR properties have been improved using dynamic vulcanisation, compatibiliser, silica and nanofiller [13–15]. Raveverma et al. [16] studied styrene-butadiene rubber (SBR)/EVA blend to produce flexible, strong and smooth FDM feedstock. Kumar et al. [9] proposed an in-house developed CNC assisted material deposition tool (MDT) to fabricate flexible parts using EVA. The developed system processes material in pellet form instead of filament, eliminating flexible parts preparation steps and buckling issues.

The present work evaluates a TPE material based on EVA/NR blends to produce flexible filament using FDM 3D printing. Two commercially grafted EVAs were used to improve EVA-NR phase interaction. The EVA and its blends were characterised based on thermal, melt flow index, mechanical, rheological and dynamic properties to understand appropriate material properties for extrusion-based additive manufacturing deposition systems using the FDM method. The FDM filament wire for selected compounds were extruded with a standard diameter of 1.75 ± 0.05 mm and tested using a 3DGence ONE 3D printer.

Experimental

Material and sample preparation

Natural rubber (SMR CV60) was purchased from KL Kepong Sdn. Bhd. Maleic anhydride grafted ethylene–vinyl acetate copolymer containing 17–20% vinyl acetate (EVA20) and 24–27% vinyl acetate (EVA24) was purchased from ARKEMA. Both materials were used as polymer matrices in this work.

EVA/NR blends were prepared at 100/0, 80/20, 70/30, 60/40 and 50/50 blend ratios. The mixing was carried out using a Haake Polylab OS Rheodrive internal mixer at a rotor speed of 60 rpm and starting temperature of 90 °C. The EVA20 or EVA24 were melt blended for 2 min before the rubber component was added. The total mixing time was 6 min.

The samples were compression moulded for 5 min in a Werner and Pfleiderer electric press at 120 °C. They were then cooled and kept under pressure for 20 min using Hexa Plast compression moulding with circulated water through the mould at 30 °C.

A roll of 1.75 mm-thick filament wire was prepared using Xplore MC 15 Micro compounder. The desired filament thickness was obtained at optimised conditions of 10 rpm rotor speed and 120 °C extrudate temperature. For the 3D printing process, a trial of EVA and its blend was printed at 190 °C using a 3DGence ONE 3D printer equipped with the 3DGence SLICER 4.0 software. The commercial 3D printing grade filaments used for comparing dynamic mechanical properties were TPU-C (Ninjaflex) and Nylon-C (PolyMide™ CoPA).

Material characterisation

Five dumbbell test pieces were stamped from a 2 mm-thick moulded sheet for tensile tests. Tensile properties were determined according to BS ISO 37:2011 (type 2 test pieces). An Instron 5564 universal testing machine with a 1 kN load cell was used with 500 mm/min cross-head speed. International Rubber Hardness Degrees (IRHD) test for hardness measurements were conducted on three rectangular samples stacked together to achieve 6 mm thickness.

A Mettler STAR^e SW 13.00 differential scanning calorimeter (DSC) was used to analyse the thermal behaviour of selected EVA/NR blends. Indium was used as reference material for temperature calibration. Approximately 5 mg of each sample were weighed and sealed in a 40-µL aluminium crucible. The DSC was programmed for a heating/cooling/heating cycle between − 120 °C and 150 °C at a rate of 20 °C/min under an oxygen-free nitrogen purge gas flow rate of 50 ml/min. For each sample, the peak temperature of melting was determined from the second heating scan.

The crystallinity (X_c) of the sample was calculated according to Eq. (1) as follows:

$$X_c = \frac{\Delta H_m}{\Delta H_0 w_{EVA}} \times 100\% \tag{1}$$

where ΔH_m is the enthalpy of fusion of the EVA samples, ΔH_0 is the enthalpy of fusion of the perfect polyethylene (PE) crystal, and w_{EVA} is the weight fraction of EVA in the polymer blend matrix. The value of ΔH_0 for PE is 277.1 J/g [17].

The melt flow index (MFI) of the blends was measured on a DYNISCO 4000 LMI indexer at 190 °C with a 2.16 kg load.

The rheological data for control material, EVA20 and EVA24 (without NR) was obtained using Xplore MC15, and the conditions are tabulated in Table 1. Melt viscosity and shear stress data at various rotor speeds (40, 60, 80 and 100 rpm) which corresponded to their respective shear rates (13, 20, 27 and 32 s^{-1}) were recorded.

A Mettler Toledo Dynamic Mechanical Thermal Analyzer (DMA1 Star system) was used for dynamic mechanical and thermal analysis. Temperature sweep measurements from − 80 to 80 ℃ were performed in tension mode at a frequency of 1 Hz and 0.1% strain with a heating rate of 5 ℃/min. The elastic/storage modulus (E'), loss modulus (E") and loss tangent (tan δ) were obtained, and the glass transition temperature (Tg) of the blends was determined as the peak position of E" when plotted as a function of temperature.

Result and discussion

Differential scanning calorimetry (DSC)

Figure 1 shows the thermal behaviour of the EVA20/NR and EVA24/NR blends from the DSC curves at 100/0, 80/20 and 70/30 blend ratios, and Table 2 summarises the corresponding data. As expected, the melting peak temperatures (T$_{m,p}$) of EVA24 were lower than EVA20 (Fig. 1a,b). Similarly, the DSC cooling curves (Fig. 1c,d) showed a lower intensity crystallisation peak for EVA24 when compared to EVA20. The crystallisation peak of EVA24 was also observed to shift to lower temperature

Table 1 Conditions for rheological data using Xplore MC15

Stages	Cumulative time, (minutes)
Volume: 15 ml	
Temperature of barrel: 120 °C	
Feed	0
Slow feeding at 70 rpm	2
After filling, blending process at a specific rotor speed	3
Extrude – filament	5
Data were averaged during a 3-min blending process	

compared to EVA20 suggesting restricted crystallisation due to the higher VA content in EVA24. This observation agrees with previous studies [17, 18]. The crystallinity (X$_c$) measurement confirmed the lower crystallinity of EVA24 than EVA20 (Table 2). Partial replacement of EVA up to 30 parts per polymer (php) NR in both EVA20/NR and EVA24/NR did not influence the T$_{m,p}$ of the blends. The X$_c$ of EVA20 and EVA24 slightly decreased with increasing NR content in the EVA/NR blends. From the DSC data in Table 2, EVA24/NR blends with blend ratio of 70/30 exhibited lower X$_c$ in comparison to EVA20 and its blends.

As EVA is a semi-crystalline polymer, it has a tendency to warp during 3D printing, therefore affecting the dimensional stability of final products [19]. Apart from selecting EVA with different VA content, introducing NR into EVA reduces crystallinity, which reduces warping tendency.

Tensile properties

Figure 2 shows the stress–strain curves of EVA20/NR and EVA24/NR, respectively, at various blend ratios. For EVA20 and EVA24, increasing NR content reduced stress and elongation at break of the blend. This result is consistent with the finding by Yong et al. [20], where the tensile strength of EVA/NR decreased as the NR content in the blends increased. The reduction of tensile strength can be explained from a morphological point of view. In this work, rubber is the minor component in the EVA/NR blends. Thus, the NR is expected to form a dispersed phase in the EVA matrix. According to the morphological study by Koshy et al. [10], NR forms a dispersed phase in the EVA matrix due to the lower NR ratio in the EVA/NR blends. Due to the low interfacial interaction between NR and EVA [20], NR acts as stress concentration points in the EVA matrix, ultimately reducing tensile strength.

Melt flow index (MFI) and hardness

Figure 3 shows the MFI of EVA/NR blends at 190 °C. The MFI of EVA20 and EVA24 blends decreased with increasing rubber content. MFI measured under specific conditions is also an indirect measurement of a polymer's molecular weight, i.e., a higher MFI value indicates a polymer with a lower molecular weight. In this case, NR has higher molecular weight than EVA and increasing NR content in an EVA/NR blend would result in greater flow resistance. Similarly, a slightly higher reduction in MFI was observed for EVA24/NR blends probably due to higher branching of EVA 24 compared to EVA20.

MFI is used in 3D printing to evaluate the ability of new materials or additives in polymer/TPE blends to flow. Wang et al. [21] identified a 10 g/10 min threshold value for PLA material for acceptable 3D printing
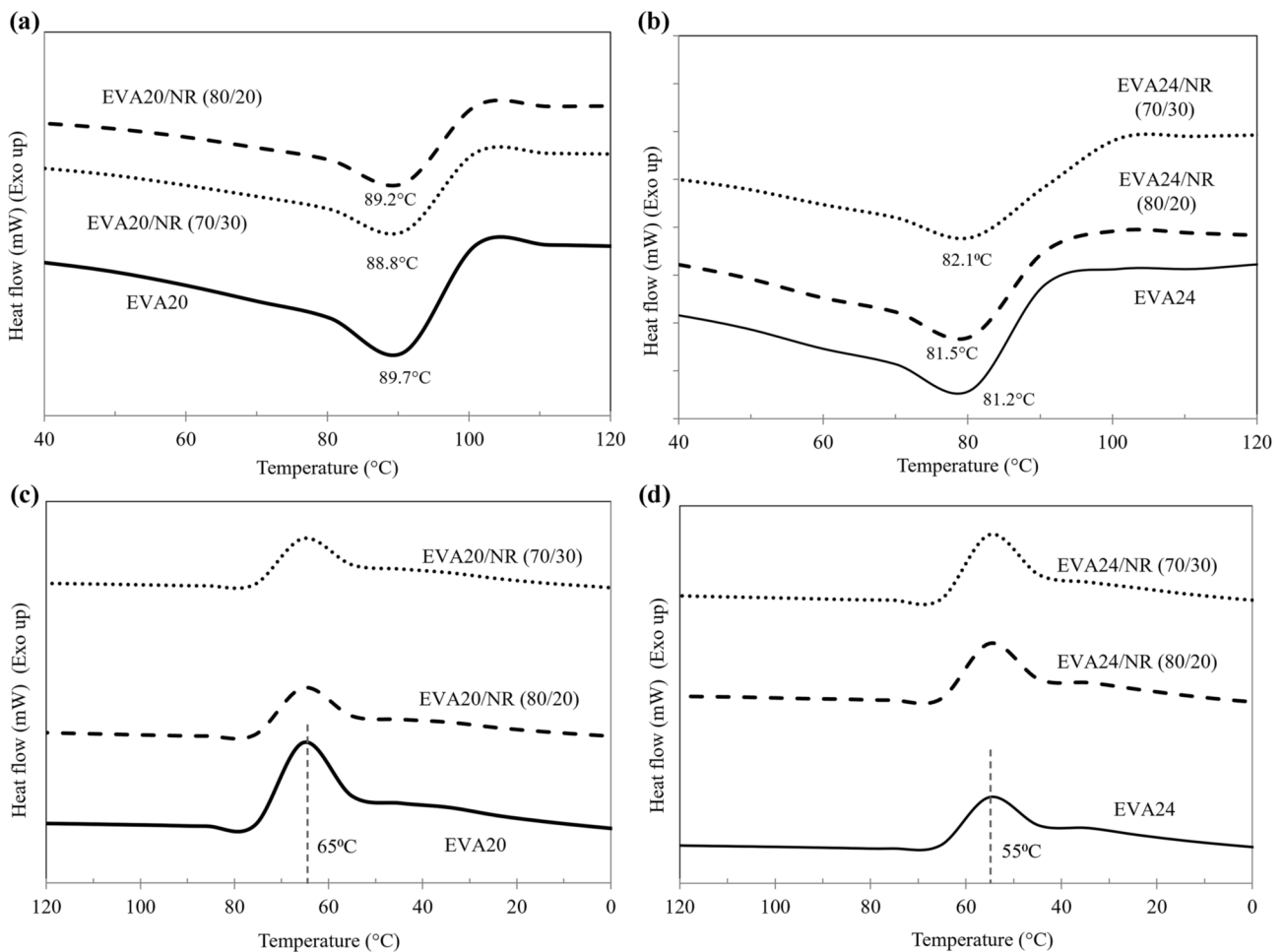
Fig. 1 DSC **a**, **b** heating and **c**, **d** cooling curves for EVA20/NR and EVA24/NR at various blend ratios indicate melting and crystallisation behaviour, respectively

Table 2 DSC characteristics data for EVA/NR at various blend ratio

EVA/NR	$T_{m,p}$ (°C)	Normalised enthalpy (J/g)	X_c (%)
EVA20/NR			
100/0	89.7	61.0	21.9
80/20	89.2	47.8	21.3
70/30	88.8	40.2	20.0
EVA24/NR			
100/0	81.2	54.9	19.8
80/20	81.5	38.2	17.6
70/30	82.1	34.1	17.2

quality. Therefore, a sufficient MFI value is required as an indicator of a suitable 3D printing material. Wang et al. [21] also highlighted the importance of interpreting MFI with additional thermal or other analysis techniques to evaluate a developed 3D printing material comprehensively. Since higher NR content caused greater flow resistance to EVA/NR blends, an EVA and EVA/NR at 80/20 blend ratio of both types were selected with the MFI value of 4–6 g/10 min at 190 °C for filament fabrication and 3D printing. It should be noted that an increase in printing temperature would affect the resulting MFI value.

A similar trend as the MFI was also observed for hardness (Fig. 4) of the blends which decreased with increasing NR content. The surface hardness of EVA copolymer is linked to VA content, molecular weight and degree of crystallinity [12]. Therefore, EVA24 exhibited lower hardness than EVA20 in the absence and presence of increasing NR content across all blend ratios. The lower hardness of the EVA24 is due to higher VA content (lower crystallinity) and increasing the NR ratio further decreased the crystallinity of the EVA phase in the blends.
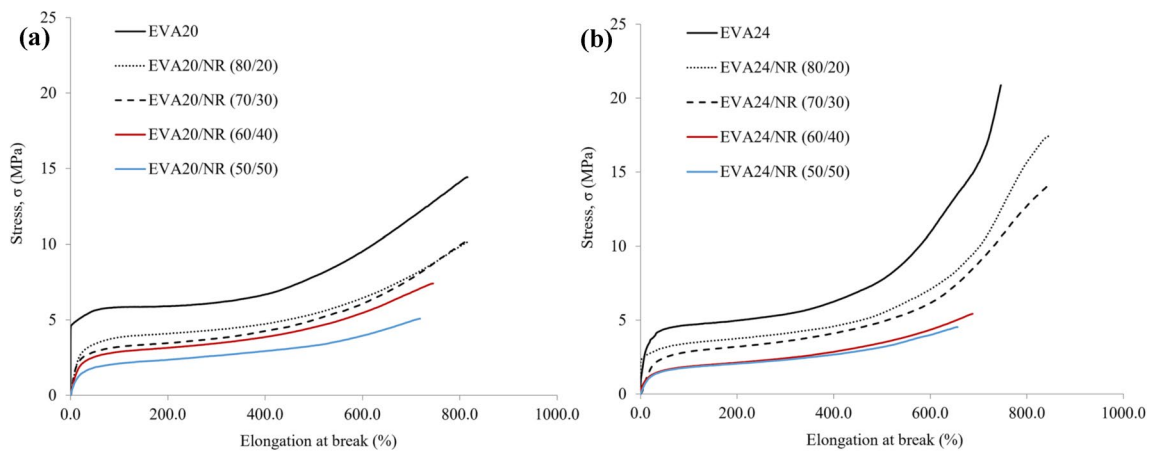
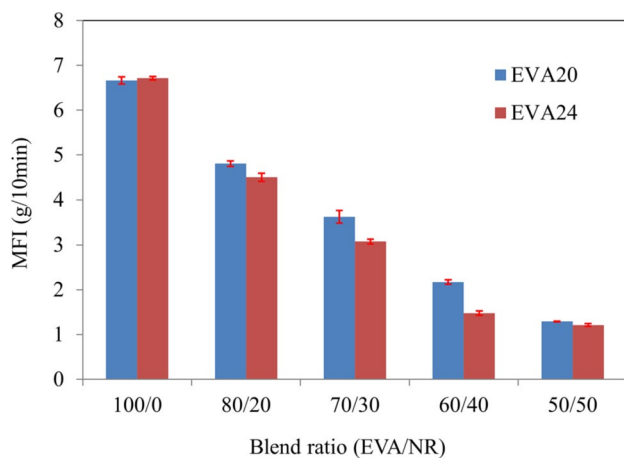**Fig. 2** Stress–strain curves of EVA/NR blends of **a** EVA20 and **b** EVA24
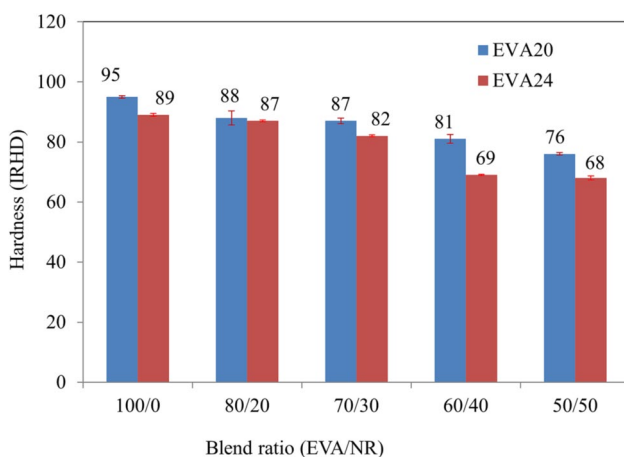

Fig. 3 MFI of EVA/NR blends

**Fig. 4** Hardness of EVA/NR blends

Printability study

A printability study was conducted to investigate the feasibility of EVA20 and its blends at 80/20 blend ratio as FDM filament at 190 °C. The blends were fabricated into filament and collected in a filament spool with thickness at 1.75 mm, as shown in Fig. 5. Therefore, the thermal properties, particularly the glass transition and melting temperatures (T_m) of the EVA20/NR blend, were used to determine the printing temperature.

In FDM 3D printing, the printed material should be heated to its T_m. It has been reported [22] that EVA containing 17–30% VA corresponds to T_m of 80–90 °C. The trend was in line with the DSC analysis, as discussed in the previous section. As EVA degrades and becomes unstable at and above 230 °C, the printing temperatures below 230 °C should be used for EVA/NR blends.

Generally, the more elastic the filaments, the more difficult it is to print, and this is true for most FDM printers. Figure 6 shows one of the trials where an EVA20 filament buckled and jammed during printing. Similarly, EVA24 and its blends experienced buckling problems due to insufficient strength and stiffness for acting as a push rod for the filament extrusion. During the 3D printing process, both strength and stiffness must be sufficient to push the melted filament during extrusion without buckling [23]. The unsuccessful 3D printing of both types of control EVAs can be explained from their rheological properties followed by the dynamic mechanical analysis of the EVA and its blend with NR.

Rheology via *Xplore MC15*

Rheology of polymer melts is often studied using a capillary rheometer to understand the flow behaviour and optimise its processing parameters. The effects of extrusion
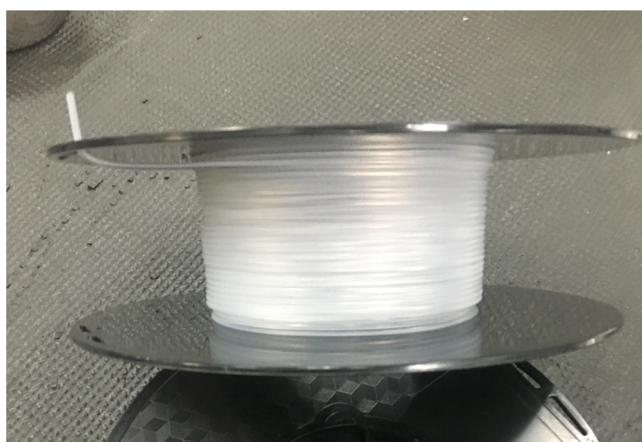
EVA20
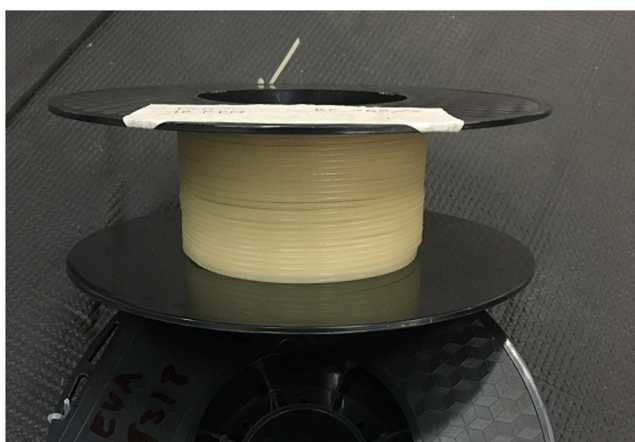
EVA20/NR (80/20)

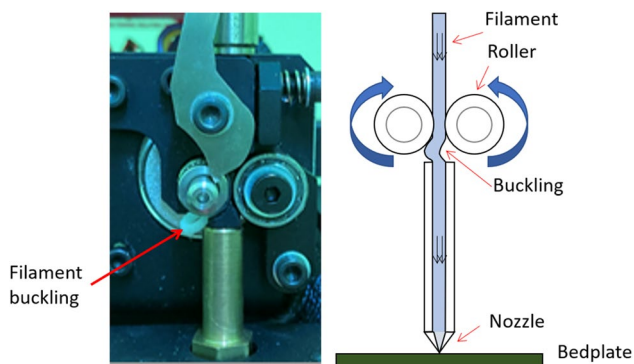**Fig. 5** Spool of filament wire ready for FDM testing

Fig. 6 Trial for sample EVA20 using 3DGence ONE 3D printer and schematic diagram of the buckling problems [23]

parameters such as shear stress, shear rate and temperature on extrusion problems (e.g., die swell, sharkskin and melt fracture) have been linked to the elastic behaviour of polymer melts during the extrusion process [24, 25]. As EVA20 and EVA24 were unsuccessfully printed using a 3DGence ONE 3D printer due to buckling problems, rheology of the control samples was evaluated using the Xplore proprietary software package of Xplore MC15 to understand the polymer flow behaviour at various rotor speeds. Figure 7 shows the melt viscosity and shear stress as a function of rotor speed at 120 °C. The temperature was selected from the optimised condition for the filament preparation.

As expected, EVA20 and EVA24 showed a reduction in the apparent melt viscosity with increasing rotor speed. The opposite was observed for shear stress which increased with increasing rotor speed. In comparison, EVA24 showed higher melt viscosity and shear stress than EVA20 due to higher VA content. Melt viscosity can be correlated to

pressure required for extrusion through the 3D printer nozzle [26]. According to Venkataraman et al. [26], buckling does not occur above a critical value and discussion on this can be found elsewhere [27]. In addition, the developed material should have sufficient viscosity to be extruded at a specific extrusion deposition temperature to retain the 3D shape. Therefore, no single factor can guarantee success in the production of flexible 3D filaments. Consequently, understanding thermal, rheological behaviour and viscoelastic properties [28] is essential for identifying the inherent material properties necessary for potential FDM feedstock.

Dynamic mechanical thermal analysis (DMTA)

Figure 8 shows the DMTA results (E', E'' and tan δ) as a function of temperature for control, EVA20/NR and EVA24/NR blends. The E' value indicates the material's stiffness. At low temperature/glassy region (below − 55 °C) EVA20 showed higher E' than EVA24. Blending of EVA20 with NR increased the E' of the EVA20/NR blends compared to respective EVA20 control polymers (Fig. 8a). Similarly, EVA24/NR (70/30) showed higher E' than EVA24. In comparison the E' of EVA20/NR (70/30) is higher than EVA24/NR (70/30). This is due to the lower VA content and higher crystallinity in the EVA20/NR blend. However, with increasing temperature, E' of the EVA/NR blends decreased drastically after reaching the crossover point of around − 55 ℃, which is the range of the glass transition temperature (Tg) of NR.

The peak of loss modulus (E'') is commonly associated with the Tg of the polymers. The single peaks at − 20 °C and − 23 ℃ for EVA20 and EVA24, respectively, reflected their Tgs. All blends exhibited two E'' peaks

Fig. 7 Melt viscosity and shear stress versus screw speeds at 120 ℃ for EVA20 and EVA24
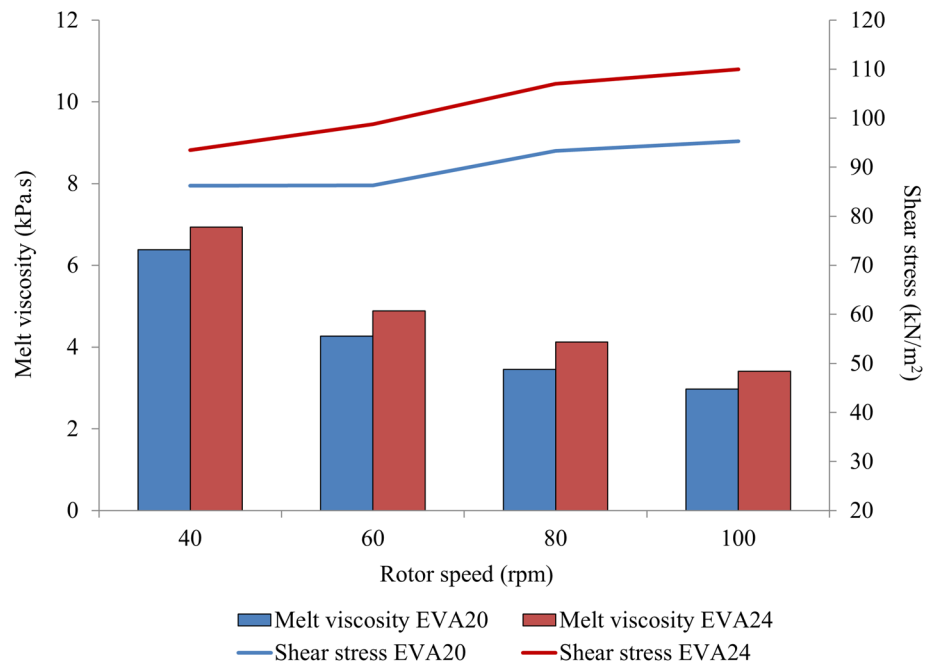
corresponding to the NR and EVA phases, indicating phase incompatibility (Fig. 8b). For EVA20/NR blend composition of 70/30, the NR was identified at the sharp peak of E'' at around − 57 °C, whereas the EVA20 peak was around − 23 ℃. For EVA24/NR at similar blend ratio, the NR and EVA24 peaks appeared at − 52 °C and − 20 °C, respectively. Compared to EVA20/NR, the E'' peak position of NR in EVA24/NR shifted towards higher temperature mainly due to chain restriction, probably resulting from physical interaction between EVA24 and NR. However, the E'' peak of EVA24 remain unchanged. The results correspond to the crystalline/amorphous component in the EVA/NR blends. The amorphous part undergoes segmental motion during the transition, whereas the crystalline region remains a crystalline solid until reaching the temperature of melting [29].

The tan δ is the ratio of the E'' to the E' and it measures energy dissipation of a material. Tan δ peak of EVA20 at − 3 ℃ shifted four degrees higher compared to EVA24 at − 7 ℃ for temperatures between − 20 to 20 ℃ due to lower VA content (Fig. 8c). In addition, the tan δ peak of EVA20 was lower and wider than EVA24 resulting from the higher crystallinity of the EVA20. The higher crystallinity of EVA20 restricts chain mobility, and, therefore, more energy is required to mobilise the molecular chains, leading to higher energy dissipation. Moreover, the tan δ peak of EVA20/NR increased with increasing NR content in the blends due to the reduction in the crystalline phase of the system as supported from the DSC results.

Figure 9 shows the E' and E'' of EVA20 and EVA20/NR blend with two commercial 3D printing filaments,

Thermoplastic Urethane (TPU-C) and Nylon (Nylon-C). Both E' and E'' of EVA20 and EVA20/NR were lower than TPU-C and Nylon-C for the whole range of temperature studied, indicating lower stiffness of EVA20 and EVA20/NR blends. Therefore, the buckling phenomena [26] of the EVA/NR blends is due to its lower stiffness and viscous response which can be associated to the final shape retention after 3D extrusion [28].

Conclusion

This work investigated the thermal, MFI, mechanical (tensile and hardness), rheology and dynamic properties of two types of grafted EVA and selected EVA/NR blend ratios. DSC results showed lower crystallinity of EVA24 and EVA24/NR blends compared to EVA20 and the corresponding blends. The MFI, tensile strength and hardness of EVA24 and EVA20 decreased as the NR component increased in the EVA/NR blends. The incompatibility of the EVA/NR blends was also evident from the DMTA analysis.

Feasibility of printing control EVAs and EVA/NR blends using FDM 3D printing technology was conducted. Two types of filaments were prepared for FDM testing. It was found that the EVA control and all the EVA/NR blends were unsuccessfully printed due to buckling attributed to the material behaviour. Firstly, the EVA and its blends experienced insufficient strength and stiffness when acting as push rods for the filament extrusion due to their low
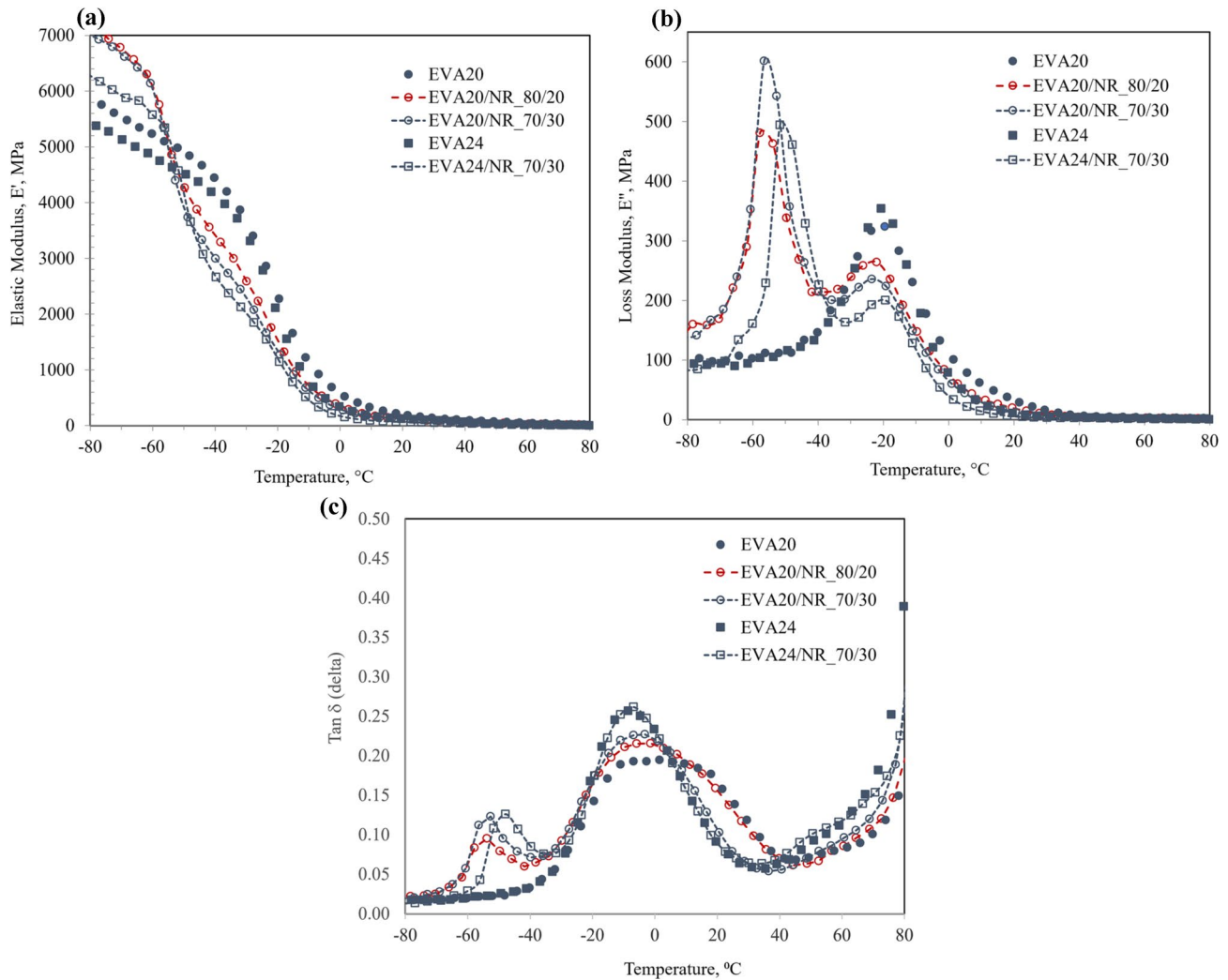
Fig. 8 Effect of temperature on the **a** elastic modulus, E', **b** loss modulus, E" and **c** tan δ of EVA20/NR and EVA24/NR blends. Frequency and strain were fixed at 1 Hz and 0.1%, respectively

stiffness indicated by the elastic modulus (E'). Secondly, the viscous response of EVA/NR blends influenced the final shape retention after 3D extrusion.

Filament buckling problems encountered for EVA/NR necessitated further revised formulation and parameter adjustments during printing. In addition, the dynamic mechanical characterisation revealed that an appropriate viscoelastic condition is required for the flexible TPE material to be successfully printed. Different thermoplastic and nano/bio fillers added to other processing ingredients can improve printability and provide desirable properties suitable for a specific application, and this can be explored in the future. The feasibility results of this work can be used as a guideline for future research into developing TPE-based flexible FDM-3D printing material, especially involving natural rubber.
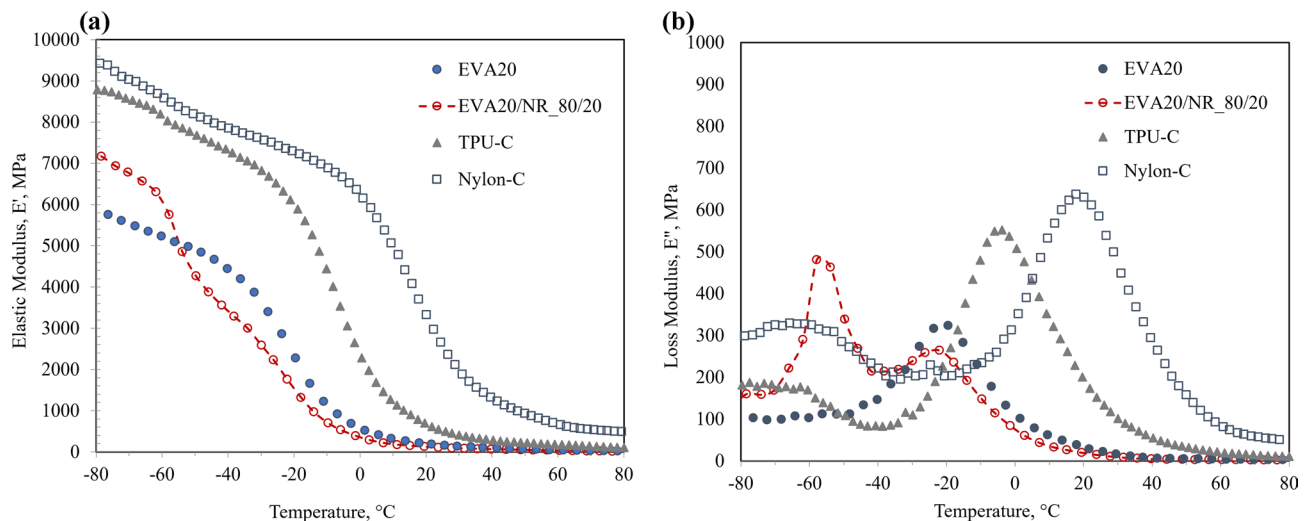
Fig. 9 Effect of temperature on the **a** elastic modulus, E', **b** loss modulus, E" of EVA20/NR blends, TPU-C and Nylon-C. Frequency and strain were fixed at 1 Hz and 0.1%, respectively

Declarations

Conflict of interest The author(s) declared no conflicts of interest with respect to the research and publication of this article.

References

1. Kazmer D (2017) Three-dimensional printing of plastics. In: Kutz M (ed) Applied plastics engineering handbook, 2nd edn. Elsevier Inc, pp 617–634

2. Przybytek A, Kucińska-Lipka J, Janik H (2016) Thermoplastic elastomer filaments and their application in 3D printing. Elastomery 20(4):32–39

3. Raveverma A, Periyasamy L (2017) The feasibility of SBR/EVA and TPU/PCL composite material for fused deposition modelling. Master Thesis, Universiti Tun Hussein Onn Malaysia

4. Lukić M, Clarke J, Tuck C, Whittow W, Wells G (2016) Printability of elastomer latex for additive manufacturing or 3D printing. J Appl Polym Sci 133(4):1–7

5. Dudek P (2013) FDM 3D printing technology in manufacturing composite elements. Arch Metall Mater 58(4):1415–1418

6. Lehmann A, Ehrmann A, Finsterbusch K (2017) Optimization of 3D printing with flexible materials. In: International textile conference, Stuttgart, Germany, 30 November–1 December 2017

7. Lay M, Thajudin NLN, Hamid ZAA, Rusli A, Abdullah MK, Shuib RK (2019) Comparison of physical and mechanical properties of PLA, ABS and nylon 6 fabricated using fused deposition modeling and injection molding. Compos B Eng 176:107341

8. Advantages and Possibilities of Soft, Elastic Materials in 3D Printing (2020). www.pollen.am. Accessed 9 Dec 2020

9. Kumar N, Jain PK, Tandon P, Mohan Pandey P (2018) 3D printing of flexible parts using EVA material. Mater Phys Mech 37(2):124–132

10. Koshy AT, Kuriakose B, Thomas S, Varhese S (1993) Studies on the effect of blend ratio and crosslinking system on thermal, X-ray and dynamic mechanical properties of blends of natural rubber and ethylene-vinyl acetate copolymer. Polym 34(16):3428–3436

11. Intharapat P (2009) Thermoplastic natural rubbers based on natural rubber (NR) and ethylene vinyl acetate copolymer (EVA) with natural rubber-graft-poly (dimethyl (methacryloyloxymethyl) phosphonate)(NR-g-PDMMMP) as compatibilizer. PhD thesis, Le Mans University

12. Henderson AM (1993) General review of ethylene-vinyl acetate (EVA) copolymer. IEEE Electr Insul Mag, AT Plastic Inc 9:3038

13. Lee J-K, Lee T-Y, Ha C-S, Lee J-O (1994) Mechanical properties of dynamically vulcanized NR and EVA blends in a roll mill. Polym Korea 18:61–61

14. Jansen P, Soares BG (1996) Effect of compatibilizer and curing system on the thermal degradation of natural rubber/EVA copolymer blends. Polym Degrad Stab 52(1):95–99

15. Ismail H, Munusamy Y, Jaafar M, Ratnam CT (2008) Preparation and characterization of ethylene vinyl acetate (EVA)/natural rubber (SMR L)/organoclay nanocomposites: effect of blending sequences and organoclay loading. Polym Plast Technol Eng 47(8):752–761

16. Raveverma P, Ibrahim M, Sa'ude N, Yarwindran M, Nasharuddin M (2017) Mechanical behaviour study on SBR/EVA composite for FDM feedstock fabrication. In: AIP Conference proceedings, Vol 1. AIP Publishing, p 020011

17. Shi XM, Zhang J, Jin J, Chen SJ (2008) Non-isothermal crystallization and melting of ethylene-vinyl acetate copolymers with different vinyl acetate contents. Express Polym Lett 2(9):623–629

18. Sefadi JS, Luyt AS (2012) Morphology and properties of EVA/empty fruit bunch composites. J Thermoplast Compos Mater 25(7):895–914

19. Spoerk M, Holzer C, Gonzalez-Gutierrez J (2020) Material extrusion-based additive manufacturing of polypropylene: a review on how to improve dimensional inaccuracy and warpage. J Appl Polym Sci 137(12):48545

20. Yong MK, Ismail H, Ariff ZM (2007) Comparison properties of natural rubber (SMR L)/ethylene vinyl acetate (EVA) copolymer

blends and epoxidized natural rubber (ENR-50)/ethylene vinyl acetate (EVA) copolymer blends. Polym Plast Technol Eng 46(4):361–366

21. Wang S, Capoen L, D'hooge DR, Cardon L, (2018) Can the melt flow index be used to predict the success of fused deposition modelling of commercial poly (lactic acid) filaments into 3D printed materials? Plast Rubber Compos 47(1):9–16

22. Adrianza JAC (2016) Thermodynamic study of the ethylene -vinyl acetate copolymer (EVA) solution separation process. PhD thesis, Universidad Complutense de Madrid.

23. Riecker S, Hein SB, Studnitzky T, Andersen O, Kieback B (2017) 3D printing of metal parts by means of fused filament fabrication — A non beam-based approach. In: International powder metallurgy congress and exhibition (Euro PM2017), Milan, Italy, 1–5 October 2017

24. Koshy AT, Kuriakose B, Thomas S, Premalatha CK, Varghese S (1993) Melt rheology and elasticity of natural rubber—ethylene-vinyl acetate copolymer blends. J Appl Polym Sci 49(5):901–912

25. Ariffin A, Ariff ZM, Jikan SS (2011) Evaluation on extrudate swell and melt fracture of polypropylene/kaolin composites at high shear stress. J Reinf Plast Compos 30(7):609–619

26. Venkataraman N, Rangarajan S, Matthewson MJ, Harper B, Safari A, Danforth SC, Wu G, Langrana N, Guceri S, Yardimci A (2000) Feedstock material property–process relationships in fused deposition of ceramics (FDC). Rapid Prototyp J 6(4):244–252

27. Turner BN, Strong R, Gold SA (2014) A review of melt extrusion additive manufacturing processes: I. Process design and modeling. Rapid Prototyp J 20(3):192–204

28. Ajinjeru C, Kishore V, Lindahl J, Sudbury Z, Hassen AA, Post B, Love L, Kunc V, Duty C (2018) The influence of dynamic rheological properties on carbon fiber-reinforced polyetherimide for large-scale extrusion-based additive manufacturing. Int J Adv Manuf Syst 99(1–4):411–418

29. George KE, Komalan C, Kumar PAS, Varughese KT, Thomas S (2007) Dynamic mechanical analysis of binary and ternary polymer blends based on nylon copolymer/EPDM rubber and EPM grafted maleic anhydride compatibilizer. Express Polym Lett 1(10):641–653